Electronic supplementary information

Remarkable self-sorting selectivity in covalently linked homochiral and heterochiral pairs driven by Pd_2L_4 helicate formation

Daiji Ogata and Junpei Yuasa*

Department of Applied Chemistry, Tokyo University of Science, 1-3 Kagurazaka, Shinjuku-ku, Tokyo 162-8601, Japan

Research Institute for Science & Technology, Tokyo University of Science, 1–3 Kagurazaka,Shinjuku-ku, Tokyo 162-8601, Japan

Experimental Section

Materials and Methods

All the chemical reagents were commercially available and used without purification. 2-iodo-1-methyl-1*H*-imidazole, (*R*)- and (*S*)-2-iodo-1-(2-methoxypropyl)-1*H*-imidazole were synthesized following procedures reported in literature.[1] ^{1}H NMR spectra were measured with JEOL JNM-ECZ400S an JNM-ECA500. UV-Vis absorption and circular dichroism (CD) spectra were recorded by an JASCO V-660 and JEOL J-725 spectrophotometer at ambient temperature, respectively. Mass spectra were measured with mass spectrometers (JEOL JMS-T100CS).

Structure Modeling.

Model structures were constructed using BIOVIA Materials Studio on molecular mechanics. The optimized structures of Pd_2L_4 were calculated with GAUSSIAN '09 on DFT-B3LYP/6-31G(d) (ligand parts); LANL2DZ (Pd^{2+}), and the relative energy level were estimated on assuming that the all isomers possess the same zero-point energy.

Nomenclature of Pd_2L_4 Self-Assembly.

In the cases of the homochiral ligand assemblies, $(Pd^{2+})_2(\mathbf{L}^{RR})_4$ and $(Pd^{2+})_2(\mathbf{L}^{SS})_4$, and the heteroligand assemblies, $(Pd^{2+})_2(\mathbf{L}^{RR})_3(\mathbf{L}^{SS})$ and $(Pd^{2+})_2(\mathbf{L}^{RR})(\mathbf{L}^{SS})_3$, only two possible isomers (*P*- and *M*-) exist, hence no specific nomenclature was used. Conversely, in the cases of the meso-ligand assemblies, $(Pd^{2+})_2(\mathbf{L}^{RS})_4$, and the meso-assemblies, $(Pd^{2+})_2(\mathbf{L}^{RR})_2(\mathbf{L}^{SS})_2$, other possible isomers (than *P*- and *M*-) present in related to the chirality at either end of the ditopic ligands, therefore specific nomenclature was used in this work. To explain the relationship at either end of the ditopic ligands, the chirality configuration was defined based on the chiral sequences of the top and bottom squares formed by the chiral groups [e.g., (*RRRS*)/(*SSSR*)].

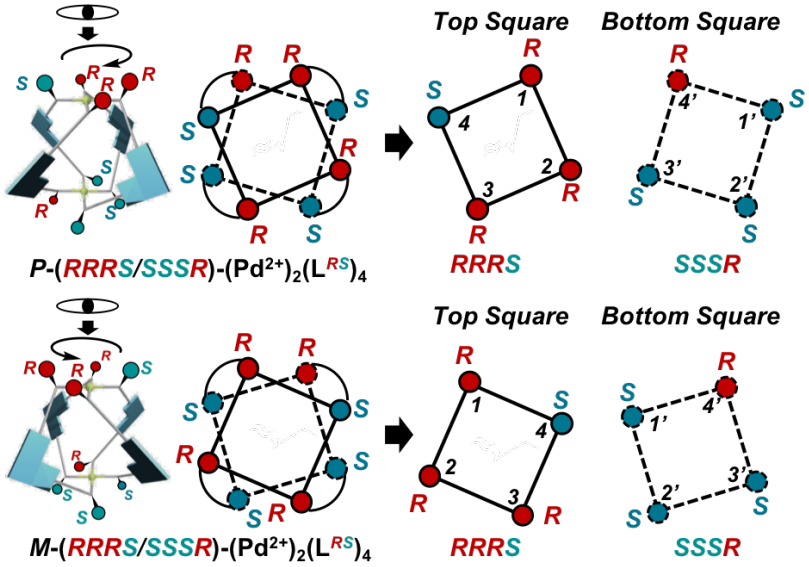

Self-Assembly Formation.

The Pd_2L_4 self-assembly processes were investigated by the CD titration experiments and ^1H NMR spectroscopy. In the case of CD measurement, $[Pd(CH_3CN)_4](BF_4)_2$ was gradually added (0.2 μM/min) to an acetonitrile solution (3 mL in 1 cm × 1 cm cuvette cell) containing the imidazole-based ditopic ligands ($\mathbf{L}^{RR}$ and $\mathbf{L}^{SS}$), while the concentration of the ligands was kept constant. ^1H NMR spectra of the Pd_2L_4 assemblies were measured as follows. After gradual addition of $[Pd(CH_3CN)_4](BF_4)_2$ (20 μM/min) to CD_3CN solution containing the imidazole-based ditopic ligands (4.0×10^{-3} M, 500 μL in NMR tube), the resulting solution was heated to 70 ˚C for 1 hour and gradually cooled to 25 ˚C in 3 hours.

Synthesis

Preparation of $(TMS)_2$Cz: To a flame-dried 200 mL two-neck flask, CuI (0.14 g, 0.74 mmol), 3,6-dibromo-9-ethyl-9*H*-carbazole (5.0 g, 14.8 mmol), THF (40 mL), and triethylamine (35 mL) were added. This solution was degassed by N_2 bubbling for 30 min. Then trimethylsilylacetylene (8.2 mL, 59 mmol), $Pd(PPh_3)_2Cl_2$ (0.51 g, 0.74 mmol) were added to the reaction flask and refluxed for 24 h under N_2 atmosphere. Then, the reaction mixture was filtered and the filtrate was evaporated. After evaporation, the crude product was purified by column chromatography on silica gel (chloroform/hexane = 2/8, R_f = 0.60). and GPC with chloroform to give 3-bromo-9-ethyl-6-((trimethylsilyl)ethynyl)-9*H*-carbazole as yellow solid (0.55 g, 10%). ^1H NMR (500 MHz, $CDCl_3$): δ 8.20 (d, J = 1.0 Hz, 2H), 7.58 (dd, J = 8.5, 1.0 Hz, 2H), 7.31 (d, J = 8.5 Hz, 2H), 4.33 (q, J = 7.5 Hz, 2H), 1.42 (t, J = 7.5 Hz, 3H), 0.29 (s, 18H).

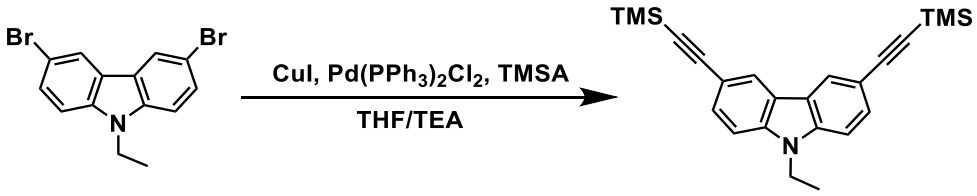

Preparation of 9-ethyl-3,6-bis((1-((*S*)-2-methoxypropyl)-1*H*-imidazol-2-yl)ethynyl)-9*H*-carbazole ($\mathbf{L}^{SS}$): To a flame-dried 100 mL two-neck flask, CuI (14 mg, 0.10 mmol), 9-ethyl-3,6-bis((trimethylsilyl)ethynyl)-9*H*-carbazole (0.60 g, 2.1 mmol), (*S*)-2-iodo-1-(2-methoxypropyl)-1*H*-imidazole (0.90 g, 4.5 mmol), THF (20 mL), and triethylamine (20 mL) were added. This solution was degassed by N_2 bubbling for 30 min. Then $Pd(PPh_3)_2Cl_2$ (54 mg, 0.10 mmol) and tetrabutylammonium fluoride (6.2 mL, 6.2 mmol) were added to the reaction flask and refluxed for 24 h under N_2 atmosphere. Then, the reaction mixture was filtered and the filtrate was evaporated. After evaporation, the crude product was purified by column chromatography on silica gel (chloroform/methanol = 9/1, R_f = 0.57) and GPC with chloroform to give 9-ethyl-3,6-

bis((1-((*S*)-2-methoxypropyl)-1*H*-imidazol-2-yl)ethynyl)-9*H*-carbazole (**L**^{SS}) as yellow solid (0.45 g, 56%). 9-ethyl-3,6-bis((1-((*R*)-2-methoxypropyl)-1*H*-imidazol-2-yl)ethynyl)-9*H*-carbazole (**L**^{RR}) was prepared using the same procedure with those of 9-ethyl-3,6-bis((1-((*S*)-2-methoxypropyl)-1*H*-imidazol-2-yl)ethynyl)-9*H*-carbazole (**L**^{SS}). ^{1}H NMR (500 MHz, $CDCl_3$): δ 8.27 (s, 2H), 7.68 (dd, J = 8.5, 1.5 Hz, 2H), 7.41 (d, J = 8.5 Hz, 2H), 7.12 (s, 2H), 7.08 (s, 2H), 4.39 (q, J = 7.5 Hz, 2H), 4.23-4.13 (m, 4H), 3.76-3.70 (m, 2H), 3.36 (s, 6H), 1.46 (t, J = 7.5 Hz, 3H), 1.23 (d, J = 6.5 Hz, 6H).

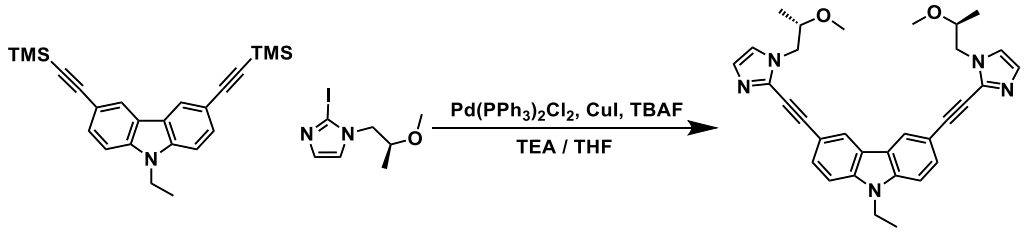

Preparation of (*S*)-3-bromo-9-ethyl-6-((1-(2-methoxypropyl)-1*H*-imidazol-2-yl)ethynyl)-9*H*-carbazole: To a flame-dried 100 mL two-neck flask, CuI (0.1 g, 0.54 mmol), 3-bromo-9-ethyl-6-((trimethylsilyl)ethynyl)-9*H*-carbazole (4.0 g, 11 mmol), (*S*)-2-iodo-1-(2-methoxypropyl)-1*H*-imidazole (3.7 g, 14 mmol), THF (30 mL), and triethylamine (30 mL) were added. This solution was degassed by N_2 bubbling for 30 min. Then $Pd(PPh_3)_2Cl_2$ (0.38 g, 0.54 mmol) and tetrabutylammonium fluoride (32 mL, 32 mmol) were added to the reaction flask and refluxed for 24 h under N_2 atmosphere. Then, the reaction mixture was filtered and the filtrate was evaporated. After evaporation, the crude product was purified by column chromatography on silica gel (chloroform/methanol = 9/1, R_f = 0.50) and GPC with chloroform to give (*S*)-3-bromo-9-ethyl-6-((1-(2-methoxypropyl)-1*H*-imidazol-2-yl)ethynyl)-9*H*-carbazole as yellow solid (2.9 g, 60%). ^{1}H NMR (300 MHz, $CDCl_3$): δ 8.22 (d, J = 1.2 Hz, 1H), 8.19 (d, J = 1.2 Hz, 1H), 7.66 (dd, J = 8.4 Hz, 1.2 Hz, 1H), 7.58 (dd, J = 8.4 Hz, 1.2 Hz, 1H), 7.38 (d, J = 8.4 Hz, 1H), 7.30 (d, J = 8.4 Hz, 1H), 7.12 (s, 1H), 7.08 (s, 1H), 4.35 (q, J = 7.2 Hz, 2H), 4.24-4.18 (m, 2H), 3.75-3.69 (m, 1H), 3.36 (s, 3H), 1.44 (t, J = 7.2 Hz, 3H), 1.16 (d, J = 7.2 Hz, 3H). ^{13}C NMR (125 MHz, $CDCl_3$) δ 140.14, 138.96, 132.60, 129.94, 129.49, 129.01, 124.33, 124.07, 123.33, 121.90, 121.34, 112.33, 112.29, 110.24, 108.93, 93.78, 77.25, 76.22, 56.84, 51.68, 37.87, 16.99, 13.76.

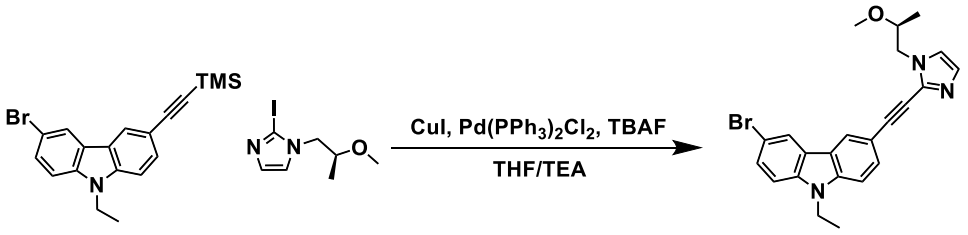

Preparation of Im^{S}(TMS)Cz: To a flame-dried 100 mL two-neck flask, CuI (62 mg, 0.33 mmol), Br(TMS)Cz (2.9 g, 6.5 mmol), (*S*)-2-iodo-1-(2-methoxypropyl)-1*H*-imidazole (1.9 g, 7.0 mmol), THF (20 mL), and triethylamine (20 mL) were added. This solution was degassed by N_2 bubbling for 30 min. Then trimethylsilylacetylene (2.7 mL, 20 mmol), $Pd(PPh_3)_2Cl_2$ (0.23 g, 0.33 mmol) were added to the reaction flask and refluxed for 24 h under N_2 atmosphere. Then, the reaction mixture was filtered and the filtrate was evaporated. After evaporation, the crude product was purified by column chromatography on silica gel (chloroform/methanol = 9/1, R_f = 0.67) and GPC with chloroform to give Im^{S}(TMS)Cz as yellow solid (0.65 g, 22%). ^{1}H NMR (400 MHz, $CDCl_3$): δ 8.24 (d, J = 1.6 Hz, 1H), 8.22 (d, J = 1.6 Hz, 1H), 7.66 (dd, J = 8.8 Hz, 1.6 Hz, 1H), 7.61 (dd, J = 8.8 Hz, 1.6 Hz, 1H), 7.38 (d, J = 8.8 Hz, 1H), 7.34 (d, J = 8.8 Hz, 1H), 7.11 (s, 1H), 7.07 (s, 1H), 4.36 (q, J = 7.2 Hz, 2H), 4.22-4.11 (m, 2H), 3.76-3.68 (m, 1H), 3.36 (s, 3H), 1.44 (t, J = 7.2 Hz, 3H), 1.22 (d, J = 7.2 Hz, 3H), 0.29 (s, 9H).

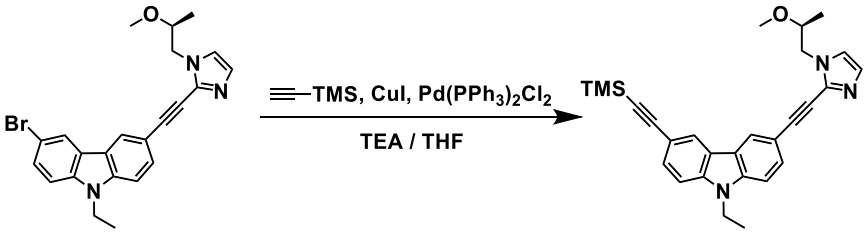

Preparation of L^{RS}: To a flame-dried 100 mL two-neck flask, CuI (13 mg, 66 μmol), Im^{S}(TMS)Cz (0.6 g, 1.3 mmol), (*R*)-2-iodo-1-(2-methoxypropyl)-1*H*-imidazole (0.42 g, 1.6 mmol), THF (20 mL), and triethylamine (20 mL) were added. This solution was degassed by N_2 bubbling for 30 min. Then $Pd(PPh_3)_2Cl_2$ (46 mg, 66 μmol) and tetrabutylammonium fluoride (4.0 mL, 4.0 mmol) were added to the reaction flask and refluxed for 24 h under N_2 atmosphere. Then, the reaction mixture was filtered and the filtrate was evaporated. After evaporation, the crude product was purified by column chromatography on silica gel (chloroform/methanol = 9/1, R_f = 0.57) and GPC with chloroform to give L^{RS} as yellow solid (0.27 g, 39%). ^{1}H NMR (500 MHz, $CDCl_3$): δ 8.28 (d, J = 1.0 Hz, 2H), 7.68 (dd, J = 8.5 Hz, 1.0 Hz, 2H), 7.41 (d, J = 8.5 Hz, 2H),

7.11 (s, 2H), 7.07 (s, 2H), 4.39 (q, J = 7.2 Hz, 2H), 4.20-4.16 (m, 4H), 3.76-3.70 (m, 2H), 3.36 (s, 6H), 1.46 (t, J = 7.5 Hz, 3H), 1.23 (d, J = 7.5 Hz, 6H). ^{13}C NMR (125 MHz, $CDCl_3$) δ 140.07, 131.91, 129.27, 128.54, 123.99, 121.88, 121.60, 111.84, 109.39, 92.76, 77.30, 75.49, 55.58, 50.71, 37.39, 15.94, 12.78.

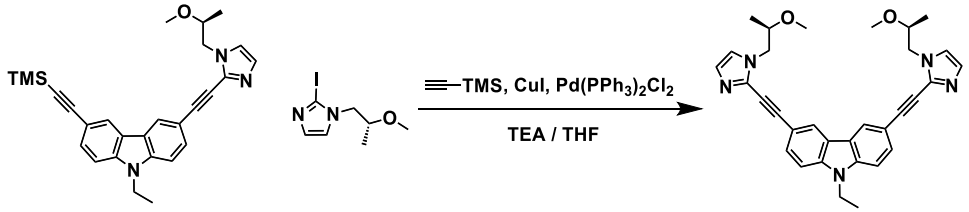

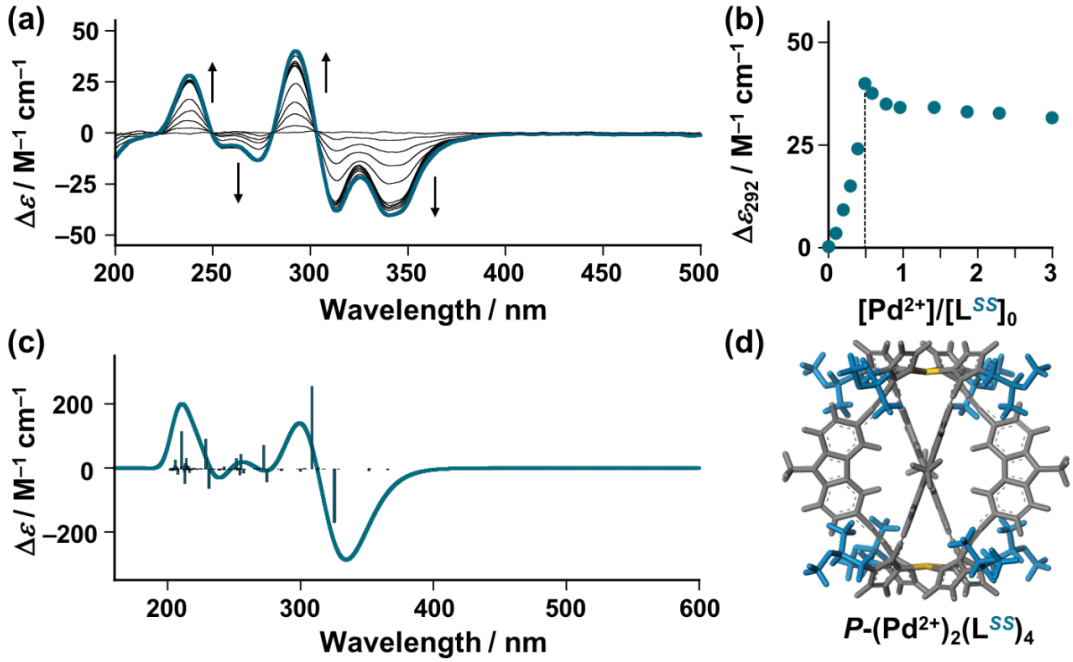

Fig. S1 (a) CD spectral changes observed during the titration of $\mathbf{L}^{SS}$ (1.9×10^{-5} M) with Pd^{2+} (0–6.1×10^{-5} M) in acetonitrile. (b) Plot of $\Delta\varepsilon$ at 292 nm vs. $[Pd^{2+}]/[\mathbf{L}^{SS}]_0$. (c) Theoretical CD spectrum [TD-DFT/CAM-B3LYP-6-31G(d)/LANL2DZ (Pd)] and (d) the optimized structure [DFT/B3LYP-6-31G(d)/LANL2DZ (Pd)] of *P*-$(Pd^{2+})_2(\mathbf{L}^{SS})_4$, where the ethyl groups at the carbazole spacers were replaced by methyl groups to reduce the calculation complexity. $\Delta\varepsilon$ [(a)-(c)] are calculated based on the concentration of $\mathbf{L}^{SS}$.

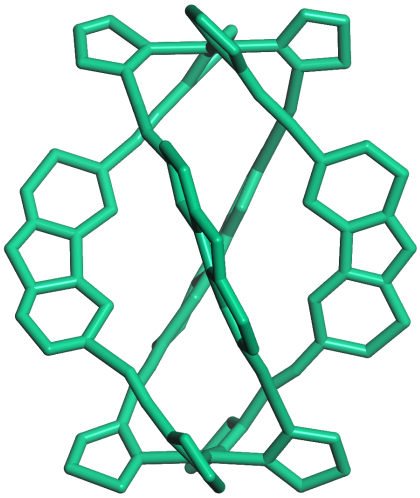

Fig. S2 Description of helix backbone geometry of $(Pd^{2+})_2(L')_4$ by referring to the X-ray crystal structure (CCDC 2008503).

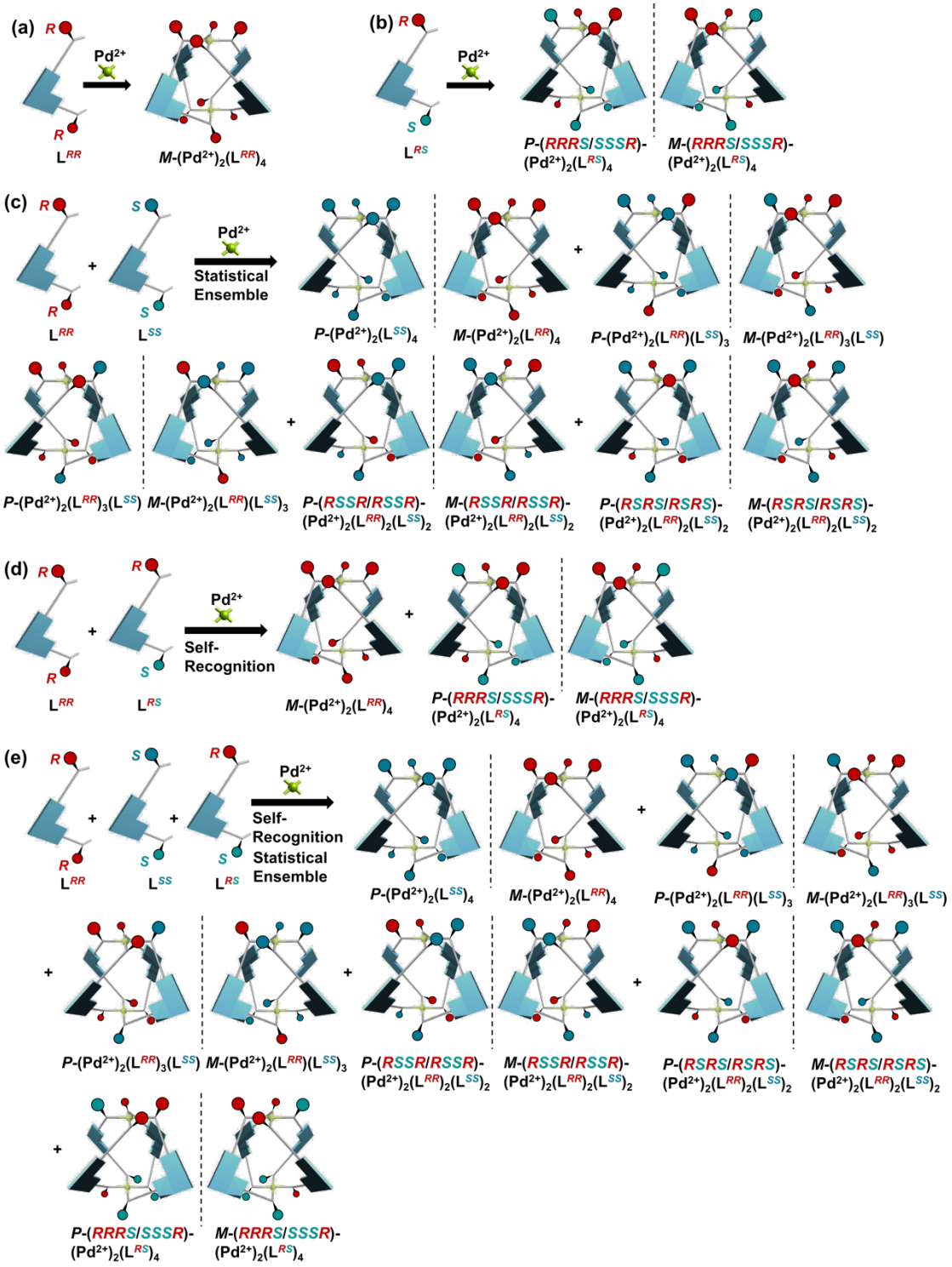

Fig. S3 Schematic representation of the Pd_2L_4 assembly formed upon addition of Pd^{2+} to (a) $\mathbf{L}^{RR}$, (b) $\mathbf{L}^{RS}$, (c) $\mathbf{L}^{RR}$ and $\mathbf{L}^{SS}$, (d) $\mathbf{L}^{RR}$ and $\mathbf{L}^{RS}$, and (e) $\mathbf{L}^{RR}$, $\mathbf{L}^{SS}$, and $\mathbf{L}^{RS}$.

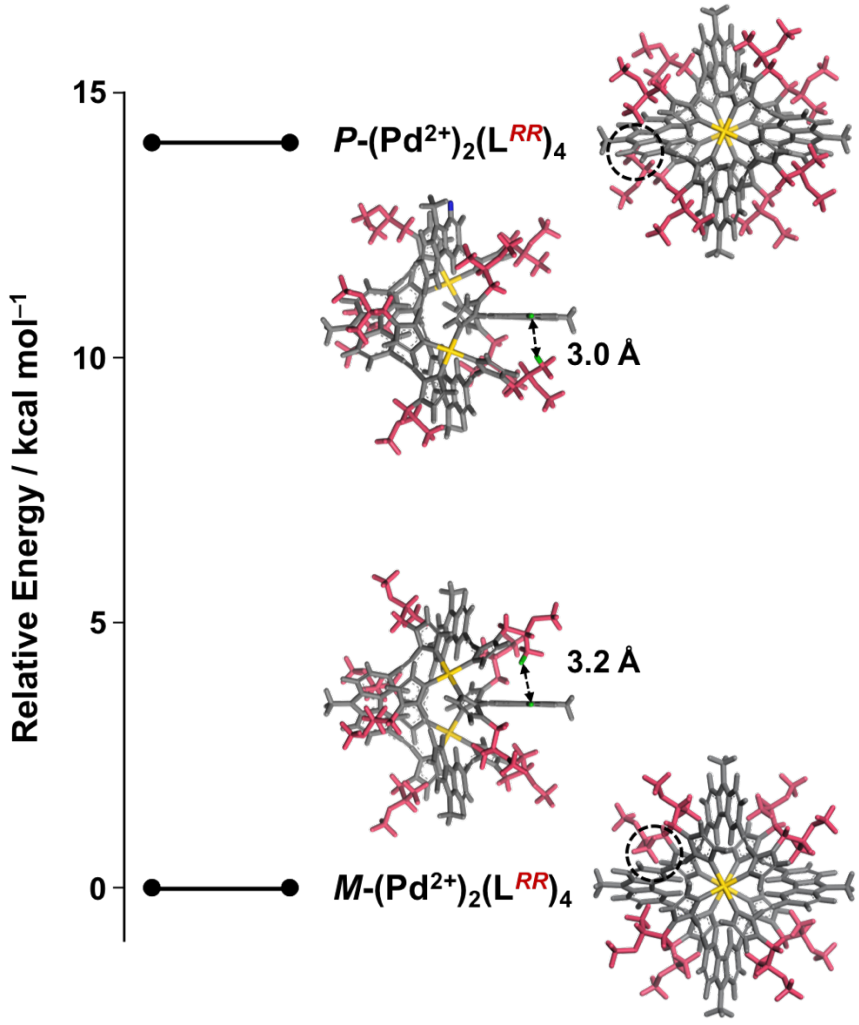

Fig. S4 Relative energy level of the optimized structures of [DFT/B3LYP-6-31G(d)/LANL2DZ (Pd)] of *M*-$(Pd^{2+})_2(\mathbf{L}^{RR})_4$ and *P*-$(Pd^{2+})_2(\mathbf{L}^{RR})_4$, where the chiral alky groups attached on the two imidazole side arms are colored in red. The DFT calculations indicate that *M*-$(Pd^{2+})_2(\mathbf{L}^{RR})_4$ is 14.06 kcal/mol lower in energy than *P*-$(Pd^{2+})_2(\mathbf{L}^{RR})_4$. This energy difference is probably arising from the difference in steric repulsion between the chiral alky groups and the helix backbone (carbazole spacers): 3.0 Å for *P*-$(Pd^{2+})_2(\mathbf{L}^{RR})_4$; 3.2 Å for *M*-$(Pd^{2+})_2(\mathbf{L}^{RR})_4$.

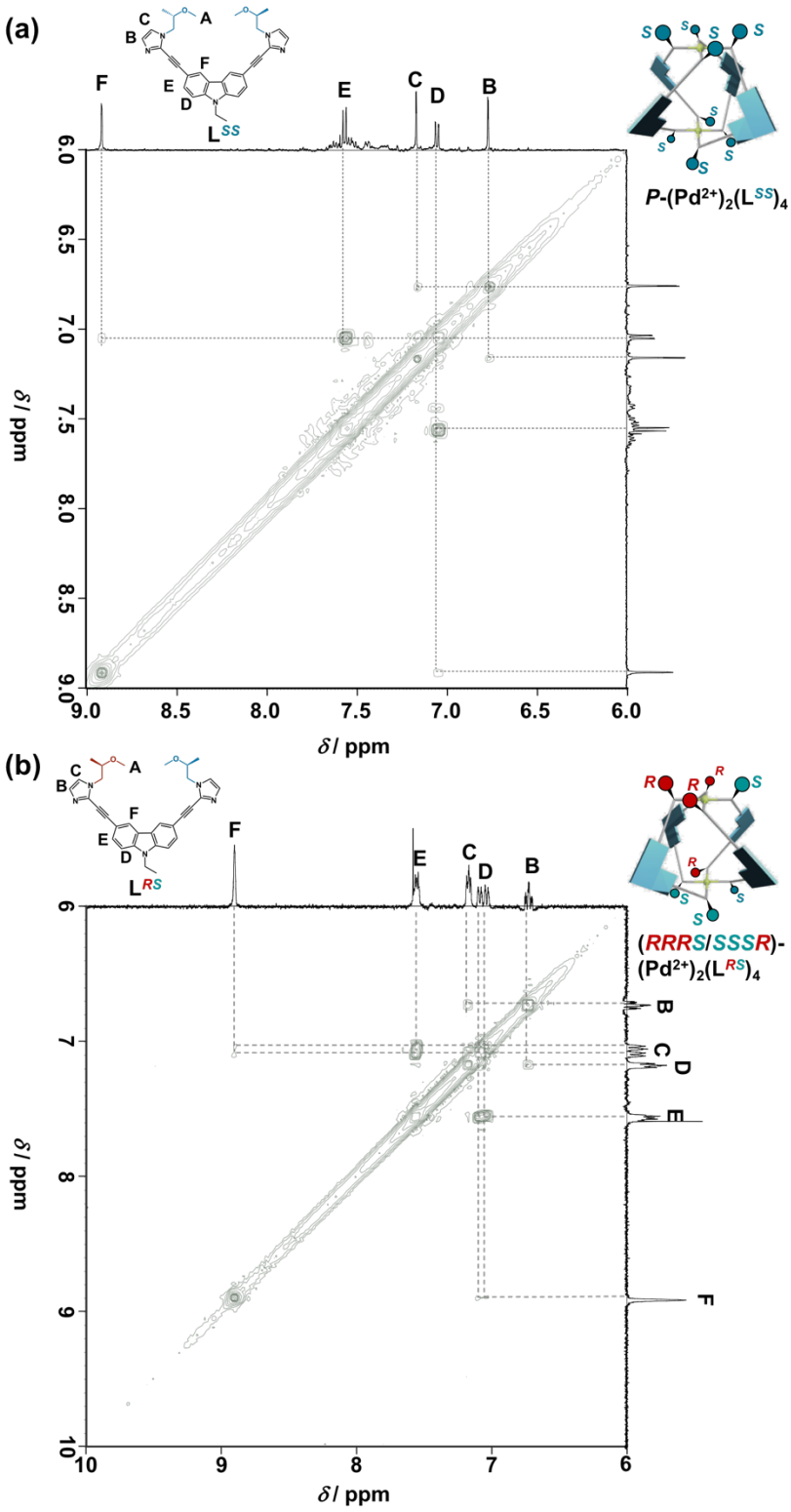

Fig. S5 ^{1}H,^{1}H-COSY NMR spectra of (a) $\mathbf{L}^{SS}$ (4.0×10^{-3} M) and (b) $\mathbf{L}^{RS}$ (4.0×10^{-3} M) in the presence of Pd^{2+} (2.0×10^{-3} M) in CD_3CN at 298 K.

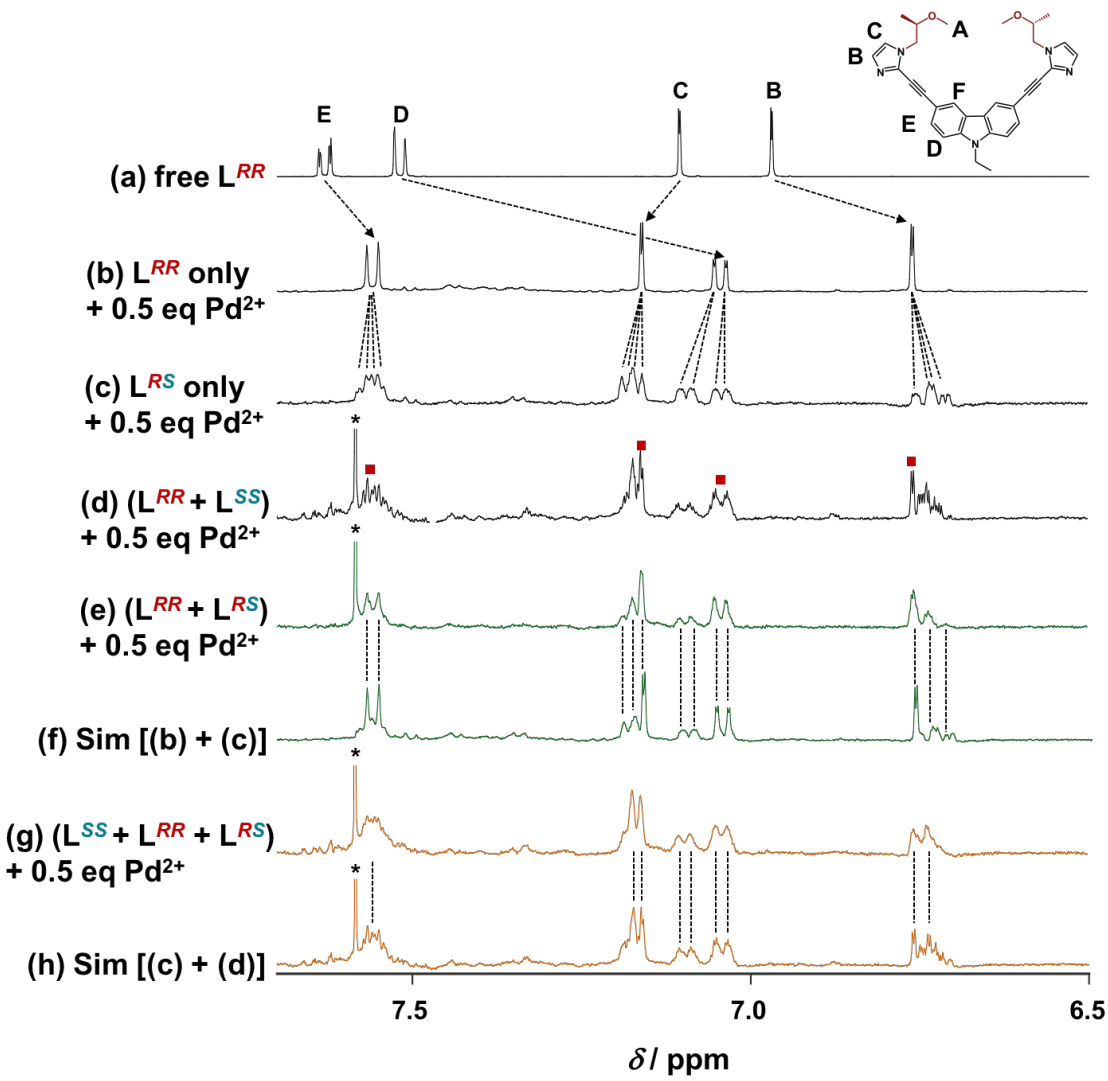

Fig. S6 (a) ^{1}H NMR spectrum of free $\mathbf{L}^{RR}$ in CD_3CN. ^{1}H NMR spectra of (b) $\mathbf{L}^{RR}$ (4.0×10^{-3} M), (c) $\mathbf{L}^{RS}$ (4.0×10^{-3} M), (d) mixture of $\mathbf{L}^{SS}$ (2.0×10^{-3} M) and $\mathbf{L}^{RR}$ (2.0×10^{-3} M), (e) mixture of $\mathbf{L}^{RR}$ (2.0×10^{-3} M) and $\mathbf{L}^{RS}$ (2.0×10^{-3} M), and (g) mixture of $\mathbf{L}^{SS}$ (1.3×10^{-3} M), $\mathbf{L}^{RR}$ (1.3×10^{-3} M), and $\mathbf{L}^{RS}$ (1.3×10^{-3} M) in CD_3CN containing 2.0×10^{-3} M of Pd^{2+} at 298 K. The chloroform peak is marked with an asterisk. The peaks marked with red squares correspond to $(Pd^{2+})_2(\mathbf{L}^{RR})_4$ and $(Pd^{2+})_2(\mathbf{L}^{SS})_4$. (f) and (h) Simulated ^{1}H NMR spectra obtained from the sum of two experimental ^{1}H NMR spectra.

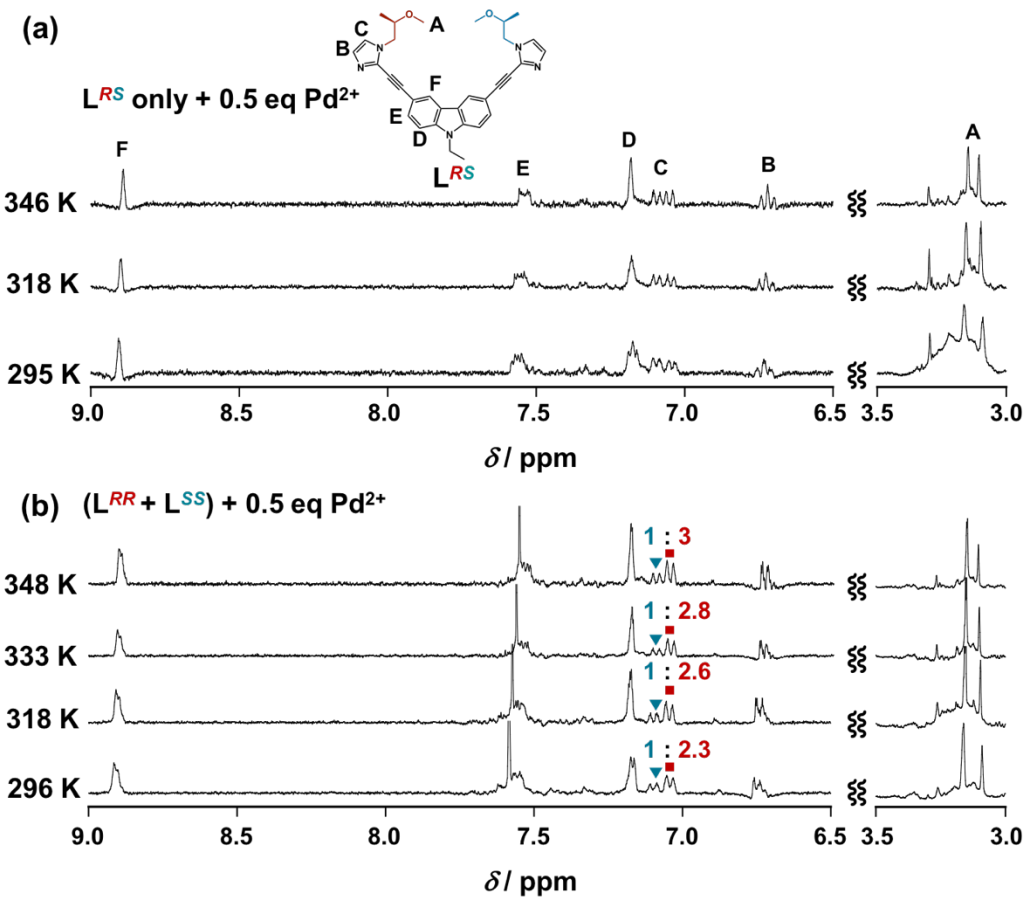

Fig. S7 ^{1}H NMR spectra of (a) $\mathbf{L}^{RS}$ (4.0×10^{-3} M) in the presence of Pd^{2+} (2.0×10^{-3} M) in CD_3CN at 295, 318, and 346 K, and those of (b) mixture of $\mathbf{L}^{SS}$ (2.0×10^{-3} M) and $\mathbf{L}^{RR}$ (2.0×10^{-3} M) in the presence of Pd^{2+} (2.0×10^{-3} M) in CD_3CN at 296, 318, 333, and 348 K.

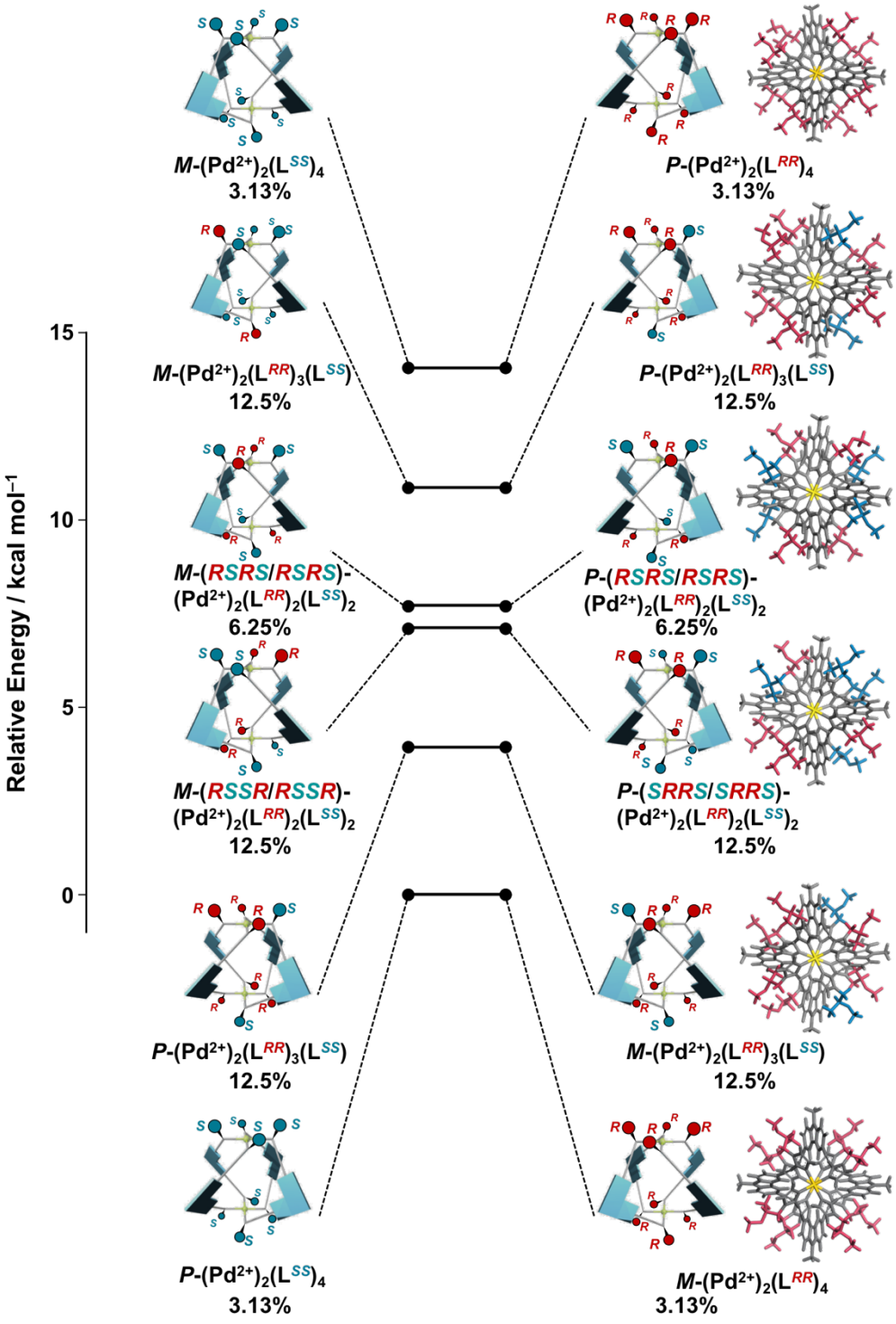

Fig. S8 Relative energy level of the optimized structures of [DFT/B3LYP-6-31G(d)/LANL2DZ (Pd)] of the possible Pd_2L_4 isomers formed upon mixing $\mathbf{L}^{RR}$ with $\mathbf{L}^{SS}$ in the presence of Pd^{2+}, where the chiral alkyl groups (*R* and *S*) attached on the two imidazole side arms are colored in red and blue, respectively; the ethyl groups at the carbazole spacers were replaced by methyl groups to reduce the calculation complexity.

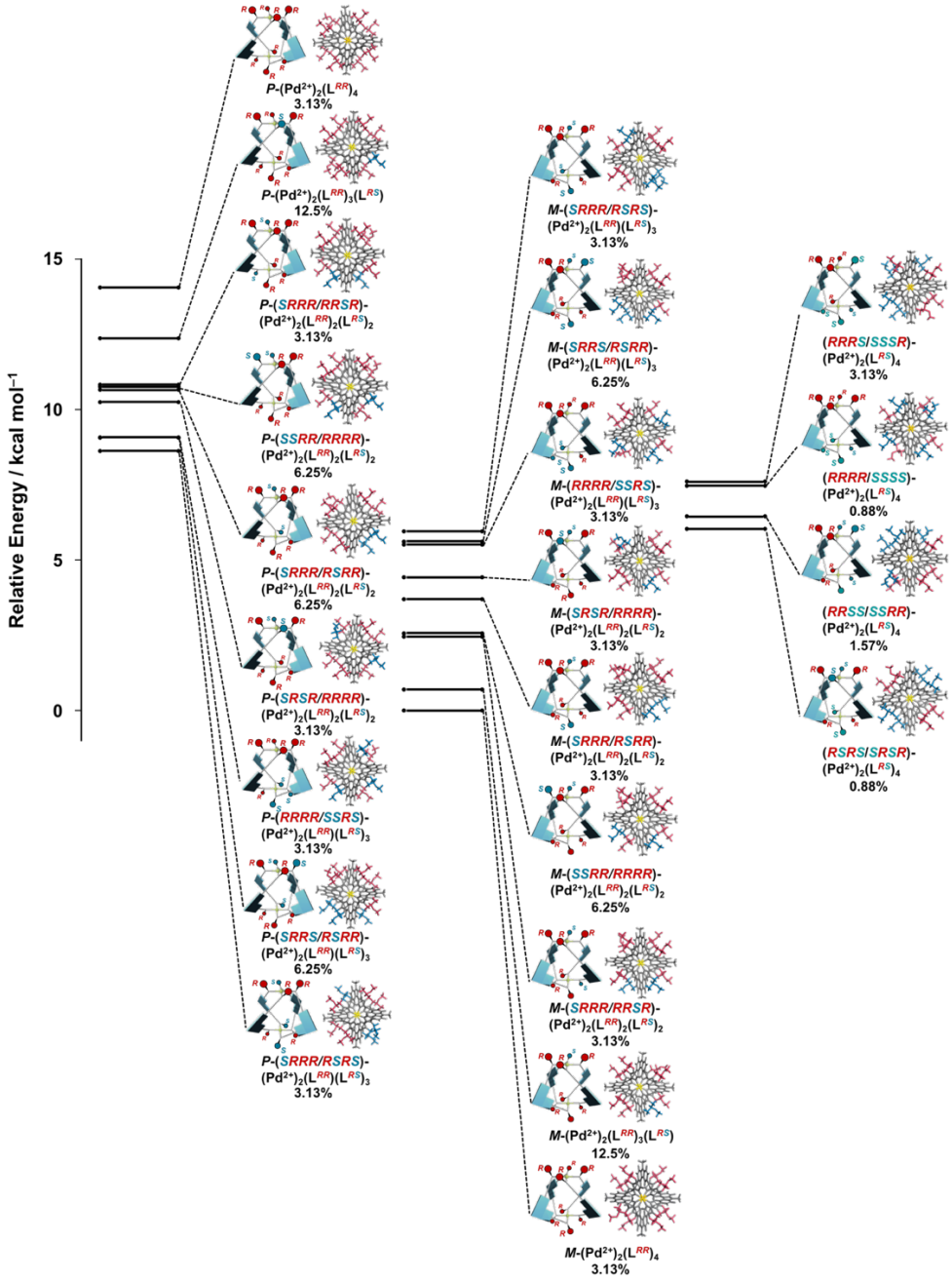

Fig. S9 Statistical probability and relative energy level of the optimized structures of [DFT/B3LYP-6-31G(d)/LANL2DZ (Pd)] for the possible Pd_2L_4 isomers formed upon mixing $\mathbf{L}^{RR}$ with $\mathbf{L}^{RS}$ in the presence of Pd^{2+}, where the chiral alkyl groups (*R* and *S*) attached on the two imidazole side arms are colored in red and blue, respectively; the ethyl groups at the carbazole spacers were replaced by methyl groups to reduce the calculation complexity.

References

(1) Ogata, D.; Yuasa, J. *Angew. Chem. Int. Ed.*, **2019**, *58*, 18424–18428.